

# Ionic exchange in groundwater hydrochemical evolution. Study case: the drainage basin of El Pescado creek (Buenos Aires province, Argentina)

Eleonora S. Carol · Eduardo E. Kruse ·  
Patricia C. Laurencena · Adolfo Rojo ·  
Marta H. Deluchi

Received: 15 April 2010 / Accepted: 12 August 2011 / Published online: 24 August 2011  
© Springer-Verlag 2011

**Abstract** The phreatic aquifer beneath the Pampean plain, in eastern central Argentina, constitutes a relevant source of water supply in the area. The objective of this work was to assess the significance of the cation exchange processes in the hydrochemical evolution of this aquifer, based on a study case located in the middle and upper basin of the El Pescado creek. Results indicate that  $\text{Ca}^{2+}/\text{Na}^+$  exchange is the main process determining the evolution of groundwater from the recharge areas ( $\text{Ca-HCO}_3$ ) towards the local discharge areas ( $\text{Na-HCO}_3$ ), as well as representing a source of  $\text{Na}^+$  contribution to the water in the aquifer. This hydrochemical characteristic is central to the identification of local discharge areas within a plain environment which extends regionally. The ion exchange capacity of these discharge areas has environmental importance, due to its influence on groundwater quality and potential groundwater uses. These results may be applied to any aquifer sharing similar hydrogeological characteristics.

**Keywords** Base exchange · Phreatic aquifer · Groundwater recharge area · Groundwater discharge area · Pampean plain

## Introduction

Ion exchange represents, together with the dissolution and alteration of minerals, one of the main processes which condition the hydrochemistry of groundwater flow (Hem 1985; Appelo and Postma 2005). In general, the surface of minerals constituting the sediments of an aquifer—especially, the clay fraction—carry negative charges, which adsorb the cations dissolved in the water. Changes in the chemical composition of water alter the equilibrium between the adsorbent phase and the solution phase, causing the adsorbed cations to be replaced by the new cations present in the water.

Numerous contributions highlight the significance of ion exchange in the chemical evolution of groundwater. A typical example of base exchange takes place in coastal aquifers affected by saltwater intrusion. The  $\text{Na}^+$  from seawater replaces the  $\text{Ca}^{2+}$  and  $\text{Mg}^{2+}$  adsorbed in the solid phase of the aquifer, producing in the mixing zone an enrichment in  $\text{Ca}^{2+}$  and  $\text{Mg}^{2+}$  (Nadler et al. 1980; Magaritz and Luzier 1985; Martínez and Bocanegra 2002; Kim et al. 2004; Rajmohan et al. 2009). This type of process may also occur when deep Na-Cl waters flow through aquifers with exchangeable  $\text{Ca}^{2+}$  (Morgan and Jankowski 2004) or when sodium waters are used to irrigate areas with exchangeable  $\text{Ca}^{2+}$  and  $\text{Mg}^{2+}$  in their soils, causing the salinization of agriculturally productive lands (Gaofeng et al. 2009; Fantong et al. 2009).

Reverse ion exchange occurs when calcium waters flow through aquifers with exchangeable  $\text{Na}^+$ -loaded clays, generating in this case an evolution from  $\text{Ca-HCO}_3$  type waters in the recharge area to  $\text{Na-HCO}_3$  type waters towards the discharge area (Coetsiers and Walraevens 2006; Nagaraju et al. 2006; Fantong et al. 2009).

In the Pampean plain, which extends over approximately 1,500,000 km<sup>2</sup> in Argentina (Fig. 1), the phreatic

E. S. Carol · E. E. Kruse (✉)  
Consejo Nacional de Investigaciones Científicas y Técnicas (CONICET), Facultad de Ciencias Naturales y Museo, Universidad Nacional de La Plata (UNLP), Calle 64 #3, 1900 La Plata, Argentina  
e-mail: kruse@fcaglp.unlp.edu.ar

P. C. Laurencena · A. Rojo · M. H. Deluchi  
Comisión de Investigaciones Científicas (CIC), Facultad de Ciencias Naturales y Museo, Universidad Nacional de La Plata (UNLP), Calle 64 #3, 1900 La Plata, Argentina

**Fig. 1** Location of the study area, sampling points and geological and groundwater flow map. *Circles* indicate sampling points in recharge areas; *triangles* indicate local discharge areas. *Dark grey area* shows post-Pampean sediment outcrops, whereas the *lighter area* shows the Pampean loess



aquifer constitutes an important source of water supply for the inhabitants of the area, as well as for agricultural and livestock farming. This aquifer is essentially composed of sandy silt sediments of eolian origin, known as the Pampean loess (loess Pampeano) (Teruggi 1957). The natural chemical quality of the water exhibits significant areal variations, as local hydrochemical behaviors associated with the groundwater flow, climatic conditions, and geomorphological variations can be identified (Bonorino et al. 2001; Quiroz Londoño et al. 2008).

The objective of this work was to assess the significance of the cation exchange processes in the hydrochemical evolution of this phreatic aquifer, based on a study case located in the middle and upper basin of the El Pescado creek in the Buenos Aires province, Argentina.

## Study area

The middle and upper basin of the El Pescado creek, which extends over a surface of approximately 400 km<sup>2</sup>, is situated in the northeast of the Buenos Aires province (Fig. 1). It is a plain drainage basin which has its sources to the south of the city of La Plata and flows into the Río de la Plata, with elevations ranging from 5 to 28 m asl. Two basic morphological features can be distinguished: the interfluvial area and the flood plain. In the interfluvial area, agricultural and livestock farming activities generally predominate, whereas in the flood plain this activity is relatively restricted. In this basin, the natural hydrological conditions are generally maintained, from both a hydraulic and a chemical point of view.

The climate is humid temperate with a mean annual rainfall of 1,060 mm. Actual evapotranspiration, obtained from the water balance at soil level (Thorntwaite and

Mather 1955), is 783 mm/year, with an estimated river runoff of 53 mm/year and an infiltration of 224 mm/year (Laurencena et al. 2005).

From a lithological perspective, the plains display homogeneous characteristics and it is possible to differentiate the sediments of the Pampean loess (Pleistocene) and the post-Pampean ones (Holocene) (Fig. 1).

The water table is located in the Pampean loess and post-Pampean sediments. The Pampean loess, which has a thickness in the order of 50 m, is composed of silt and sandy silt of eolian origin containing plagioclase, volcanic glass, and calcareous carbonates. The post-Pampean sediments, of fluvial estuarine or marine origin, are constituted by clayey silt and clay (illite and smectite) and have a thickness of up to 5 m.

The Pampean loess is underlain by sandy sediments of fluvial origin, known as the Arenas Puelches (Puelches sands), with a thickness of 20 m; it constitutes a highly productive low salinity semi-confined aquifer. The Pampean loess and the Arenas Puelches are separated by a clayey layer with a thickness that may reach 10 m, which determines the hydraulic interrelationship between the aquifers.

The El Pescado creek exhibits its effluent behavior with respect to the water table practically along its entire course (Fig. 1). The interfluvial area is predominantly a recharge zone, with a water table depth which varies between 5 and 15 m below ground surface (bgs). Local groundwater flows towards the flood plain, where water table depths vary between 1 and 2 m bgs, with the discharge taking place in the watercourse. The regional groundwater flows in a north-eastward direction and hydraulic gradients vary between 1.8 and 0.5 m/km (Kruse et al. 2003). There is no intensive local exploitation of the groundwater system in this basin.

In the interfluvial recharge zone, there is a downward vertical flow from the phreatic aquifer to the semi-confined aquifer, as well as lateral flow within the phreatic aquifer. In the discharge areas, i.e., in the flood plain, the hydrogeological and hydraulic conditions rule out the possibility of upward vertical flow from the semi-confined to the phreatic aquifer. Therefore, the phreatic aquifer is the upper portion of a multilayer groundwater system (Sala and Auge 1973), which is recharged by the infiltration of the water balance surplus.

## Methodology

The hydrochemical data, which were derived from sampling a groundwater-monitoring network, established in the study area, were interpreted (Fig. 1).

In the water samples, pH, conductivity, calcium, magnesium, sodium, potassium, chloride, sulphate, carbonate and bicarbonate were determined. The collection, preservation, and chemical analysis of the water samples were carried out according to the methods recommended by the American Public Health Association (APHA 1998). Sodium ( $\text{Na}^+$ ) and potassium ( $\text{K}^+$ ) were determined by means of flame photometry. Hardness as calcium carbonate ( $\text{CaCO}_3$ ), calcium ( $\text{Ca}^{2+}$ ), carbonate ( $\text{CO}_3^{2-}$ ), bicarbonate ( $\text{HCO}_3^-$ ) and chloride ( $\text{Cl}^-$ ) were estimated by volumetric methods. Magnesium ( $\text{Mg}^{2+}$ ) was calculated from the levels of total hardness and calcium, whereas sulphate ( $\text{SO}_4^{2-}$ ) was measured by nephelometry. Electric conductivity and pH were determined in the field immediately after the collection of the sample using a portable equipment.

Results concerning major-ion concentrations were analyzed by means of hydrochemical charts and hydrogeochemical modeling using the NETPATH software (Plummer et al. 1991). The determination of soluble ionic species and saturation indices (SI) was carried out by means of the PHREEQC software (Parkhurst and Appelo 1999).

## Results

Phreatic water is characterized by its low salt content with frequent conductivity values below 1,200  $\mu\text{S}/\text{cm}$  (Table 1). In the recharge areas, water is Ca– $\text{HCO}_3$  type (Fig. 2), with  $\text{HCO}_3^-$  and  $\text{Ca}^{2+}$  contents varying from 476 to 659 mg/L and from 46 to 106 mg/L, respectively (Table 1). In the local discharge areas, water is Na– $\text{HCO}_3$  type (Fig. 2) with  $\text{HCO}_3^-$  concentration ranging from 494 to 738 mg/L, whereas  $\text{Na}^+$  concentration varies between 134 and 289 mg/L (Table 1). The  $\text{Cl}^-$  and  $\text{SO}_4^{2-}$  contents are low

in both areas, with frequent values below 70 mg/L. The  $\text{Mg}^{2+}$  content varies between 28 and 51 mg/L in the recharge area, and between 9 and 41 mg/L in the discharge area; whereas the concentrations of  $\text{K}^+$  are low in both areas, usually below 13 mg/L (Table 1).

A pH increase from 7.3 to 8.1 can be observed from the recharge areas towards the local discharge areas. The contents of  $\text{HCO}_3^-$  do not vary significantly when pH increases, whereas  $\text{Ca}^{2+}$  decreases (Fig. 3a, b). An excess of  $\text{HCO}_3^-$  with respect to  $\text{Ca}^{2+}$  can be observed, with all the samples lying below the 1:1 line in the graph of  $\text{Ca}^{2+}$  versus  $\text{HCO}_3^-$  (Fig. 3d).

The  $\text{Na}^+/\text{Cl}^-$  ratio decreases from 14.8 to 1.0 as the content of  $\text{Ca}^{2+}$  increases (Fig. 3c). The highest  $\text{Na}^+/\text{Cl}^-$  values were recorded in the samples of the discharge area, which would indicate an excess of  $\text{Na}^+$  in these sections of the basin.

The  $\text{Na}^+ - \text{Cl}^-$  values vary between 0.47 and 10.77, suggesting an excess of  $\text{Na}^+$ , whereas  $(\text{Ca}^{2+} + \text{Mg}^{2+}) - (\text{SO}_4^{2-} + \text{CO}_3^{2-} + \text{HCO}_3^-)$  varies between 0.30 and 10.66, indicating a deficiency in  $\text{Ca}^{2+} + \text{Mg}^{2+}$ . These excesses and deficiencies have a linear relationship close to 1 with a correlation coefficient ( $r^2$ ) of 0.94 and they are larger in the local discharge area samples than in the recharge ones (Fig. 3e). Another sign of  $\text{Na}^+$  excess is the negative values (between  $-0.08$  and  $-14.20$ ) in the  $\text{Cl}^- - (\text{Na}^+ + \text{K}^+)/\text{Cl}^-$  ratio, with the most negative values being recorded in the discharge area, associated with the lowest  $\text{Ca}^{2+} + \text{Mg}^{2+}$  concentrations (Fig. 3f).

The SI with respect to calcite show undersaturated values in the recharge and discharge areas of the upper basin and supersaturated ones in the discharge area of the middle basin. In turn, all samples were undersaturated with respect to gypsum, with SI values below  $-2.1$  (Fig. 4)

## Discussion

By means of the study of ionic ratios, it is possible to recognize the geochemical processes that determine the chemical composition of groundwater. Therefore, it is necessary to understand the hydrodynamics of groundwater (type of recharge, connection with other aquifers or surface water inflow, etc.) and the mineralogy of the aquifer. Through hydrogeochemical modeling it is also possible to verify if the processes defined by the ionic ratios are thermodynamically and stoichiometrically correct.

The phreatic aquifer is recharged by the rainfall surplus of the water balance and does not receive groundwater inflow from the underlying aquifer units. Therefore, the groundwater chemistry is determined by the chemical reactions occurring during rainfall infiltration and groundwater flow. Infiltration-related processes dominate the

**Table 1** Hydrochemical data from groundwater

Sample	EC	pH	HCO <sub>3</sub> <sup>-</sup>	SO <sub>4</sub> <sup>2-</sup>	Cl <sup>-</sup>	Ca <sup>2+</sup>	Mg <sup>2+</sup>	Na <sup>+</sup>	K <sup>+</sup>
Recharge									
R1	1,095	7.3	616	32	60	97	43	125	9.7
R2	1,262	7.5	659	27	89	49	42	189	12
R3	1,100	7.8	531	22	71	88	51	88	19.2
R4	1,352	7.5	543	61	142	106	29	176	11.2
R5	1,884	7.6	482	37	358	105	38	243	11.2
R6	920	7.6	555	13	64	66	28	130	9.7
R7	754	7.7	476	15	35	46	30	102	13.2
Local discharge									
D1	734	7.9	494	7	14	25	22	134	6.7
D2	855	8.1	537	18	21	26	17	193	5.6
D3	1,035	7.9	579	31	67	22	21	218	7.6
D4	740	7.9	525	9	32	18	9	178	5.6
D5	1,000	7.9	525	13	46	34	23	187	12.1
D6	827	8.1	535	11	35	18	11	208	6.1
D7	719	8.1	531	11	21	14	8	182	5.7
D8	690	8.1	512	9	18	23	20	139	11.6
D9	1,284	7.7	689	75	57	41	41	248	38.5
D10	1,200	8.0	738	51	64	22	17	289	6.6
D11	850	7.8	549	19	35	32	19	173	10.1
D12	853	8.0	567	13	28	23	15	195	4.6
Rainwater	57	7.2	51	7	17	4	4	13	–

Electrical conductivity in  $\mu\text{S}/\text{cm}$  and major ions in  $\text{mg}/\text{L}$ . Rainfall data correspond to mean values recorded in the area

**Fig. 2** Piper diagram for groundwater samples. Symbols as in Fig. 1

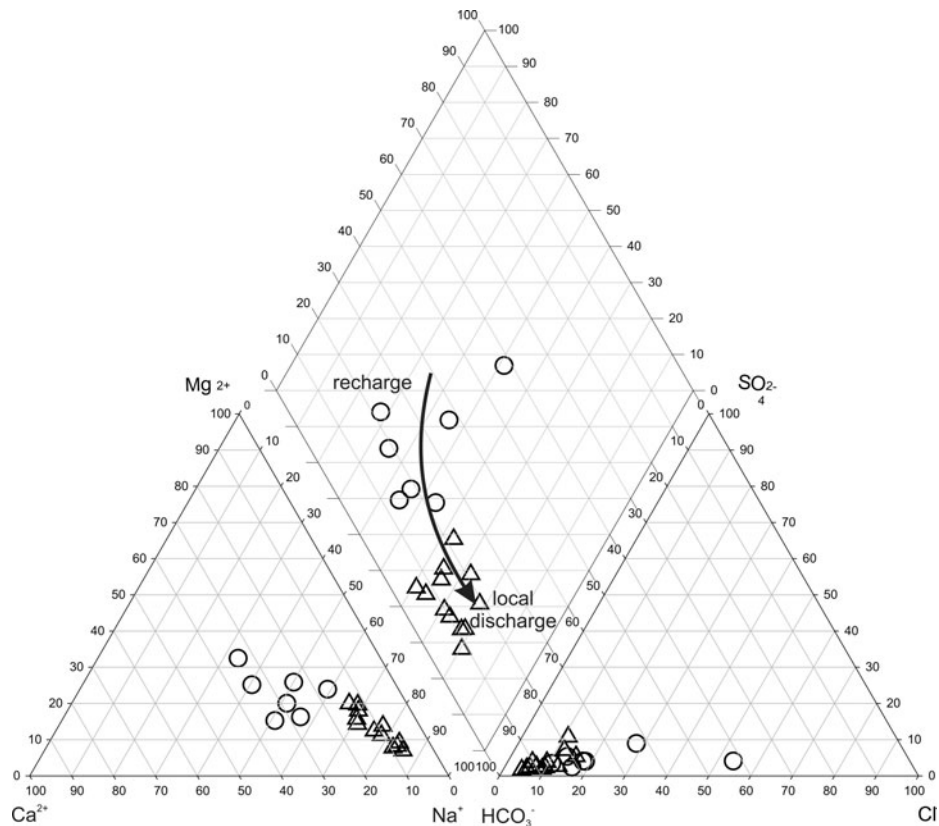
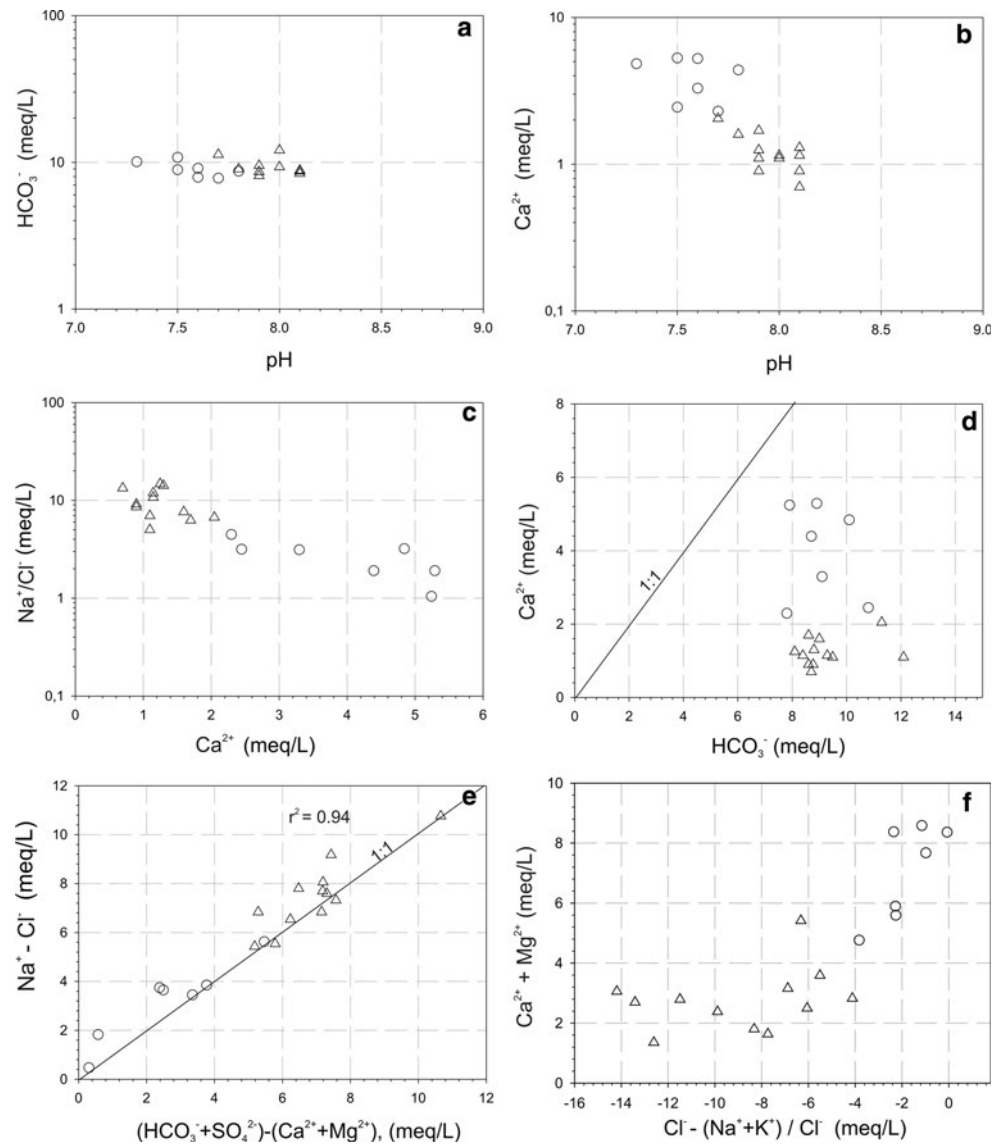


**Fig. 3** Hydrochemical relationships between selected ions. Symbols as in Fig. 1



recharge areas (i.e., the Pampean loess). The evolution observed from Ca–HCO<sub>3</sub> to Na–HCO<sub>3</sub> facies from the recharge areas to the discharge areas is the result of processes occurring during groundwater flow between the Pampean loess and the post-Pampean sediments. The mineralogical characteristics of these sediments and their relationship with the ions studied suggest that the predominance of calcium carbonate in the recharge area and of clays (illite and smectite) in the discharge area constitute the most relevant reactive phases.

Rainwater dissolves atmospheric CO<sub>2(g)</sub> and as it infiltrates the soil it incorporates the CO<sub>2(g)</sub> which is trapped in the pore spaces, mainly in the areas with root growth and the presence of decomposing organic matter. The CO<sub>2(g)</sub> reacts with the water to form H<sub>2</sub>CO<sub>3</sub>, which first dissociates into HCO<sub>3</sub><sup>-</sup> and H<sup>+</sup> ions, and then HCO<sub>3</sub><sup>-</sup> into CO<sub>3</sub><sup>2-</sup> + H<sup>+</sup>, with HCO<sub>3</sub><sup>-</sup> being the dominant species in the pH values

ranging from 6.5 to 10 (Appelo and Postma 2005). The protons released are consumed by carbonate dissolution (HCO<sub>3</sub><sup>-</sup> + H<sup>+</sup> + CaCO<sub>3</sub> ↔ Ca<sup>2+</sup> + 2HCO<sub>3</sub><sup>-</sup>). In the unsaturated zone (USZ), which is an open system with respect to CO<sub>2(g)</sub>, the protons consumed in the carbonate dissolution are regenerated due to the dissolution of the CO<sub>2(g)</sub> available in the sediment pores. When the infiltrating water enters the saturated zone, which is a closed system with respect to CO<sub>2(g)</sub>, the protons consumed cannot be regenerated, as in this area there is no CO<sub>2(g)</sub> available in the system. Therefore, the water flowing through the aquifer has pH values slightly over 7, and in the direction of the groundwater flow (i.e., from the recharge areas towards the discharge ones) water pH tends to increase as the carbonate phases become altered, yielding values between 7.3 and 7.8 in the recharge areas, and 7.7 and 8.1 in the discharge ones (Table 1). The SI also shows a relationship between



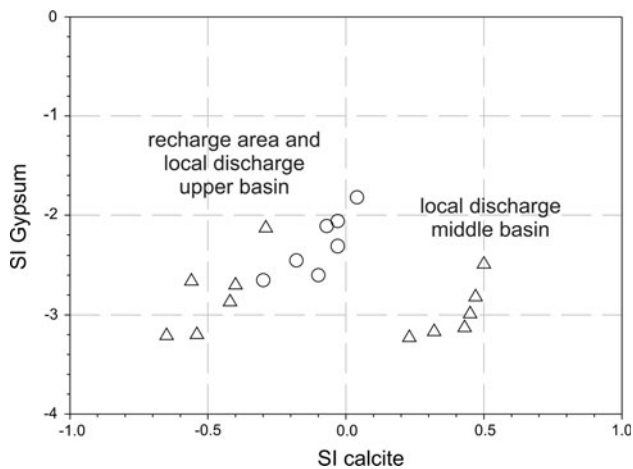


**Fig. 4** Saturation indices. Symbols as in Fig. 1

groundwater flow and carbonate dissolution. In the recharge and local discharge areas of the upper basin, water is undersaturated with respect to calcite (Fig. 4) and may dissolve the calcium carbonate in the sediments. In the local discharge areas of the middle basin, where post-Pampean sediments become more developed, water is supersaturated with respect to calcite (Fig. 4), a condition that favors the precipitation of calcium carbonate. In turn, the slight variation in  $\text{HCO}_3^-$  content accompanying the increase in pH (Fig. 3a) is associated with the  $\text{CO}_{2(g)}$  dissolution and infiltration processes occurring throughout the basin, as it is a phreatic aquifer. The contribution of  $\text{HCO}_3^-$  from two sources (infiltration and carbonate dissolution) produces  $\text{Ca}^{2+}$  defects with respect to  $\text{HCO}_3^-$  (Fig. 3d). This indicates that the Ca– $\text{HCO}_3$  character of groundwater in the recharge area mainly derives from the contribution of  $\text{HCO}_3^-$  originated from  $\text{CO}_{2(g)}$  dissolution during rainwater infiltration and by the  $\text{HCO}_3^-$  and  $\text{Ca}^{2+}$  arising as a result of carbonate dissolution.

The low content of  $\text{SO}_4^{2-}$  (generally below 0.8 meq/L) and  $\text{Cl}^-$  (below 4.0 meq/L, except for one sample), and the absence of minerals such as  $\text{CaSO}_4$  and  $\text{NaCl}$  among the components of the solid phase of the aquifer indicate that the main source of chlorides and sulphates dissolved in the groundwater is rainwater evaporation.

Towards the local discharge areas, this  $\text{Ca}^{2+}$  defect increases and it is accompanied by a marked excess of  $\text{Na}^+$  (Fig. 3c). The larger contribution of  $\text{Na}^+$  with respect to

$\text{Ca}^{2+}$  over the total number of cations is an indication of the influence of the ion exchange (Hem 1985). The low contents of  $\text{Ca}^{2+} + \text{Mg}^{2+}$  (below 4 meq/L), associated with negative values of  $\text{Cl}^-(\text{Na}^+ + \text{K}^+)/\text{Cl}^-$  and a value of  $-0.94$  as a result of the ratio between  $(\text{Na}^+ - \text{Cl}^-)$  and  $(\text{Ca}^{2+} + \text{Mg}^{2+}) - (\text{SO}_4^{2-} + \text{CO}_3^{2-} + \text{HCO}_3^-)$  (Fig. 3e, f), confirm the importance of this process (McLean et al. 2000) in the hydrochemical evolution from recharge to local discharge areas.

The discharge area samples also show higher  $\text{Na}^+/\text{Cl}^-$  values associated with low contents of  $\text{Ca}^{2+} + \text{Mg}^{2+}$  (Fig. 3c) and higher excess of  $\text{HCO}_3^-$  with respect to  $\text{Ca}^{2+} + \text{Mg}^{2+}$  (Fig. 3d) than the recharge area samples. These two characteristics are consistent with a process of  $\text{Ca}^{2+}/\text{Na}^+$  exchange (Tijani 2004). The  $\text{Ca}^{2+}$  incorporated to water—mainly as a result of the dissolution of the carbonates present in loess sediments—is exchanged by the  $\text{Na}^+$  adsorbed in the clayey sediments associated with post-Pampean sediments (alkaline soils) in the local discharge areas. In this manner, the Ca– $\text{HCO}_3$  type groundwater of the recharge area becomes a Na– $\text{HCO}_3$  type water in the discharge sites.

In order to test the processes determined by means of the assessment of ionic ratios, a hydrogeochemical model was made using the NETPATH software (Plummer et al. 1991). In the first place, the geochemical evolution in recharge areas was analysed, based on rainwater infiltration into the loess sediments, using the average chemical composition of rainwater in the area (Table 1). Results indicate that as the rainwater infiltrates, it dissolves  $\text{CO}_{2(g)}$  (between 0.06 and 0.63 mmol/L) and carbonates (between 0.16 and 0.21 mmol/L). The thickness of the USZ in the recharge areas varies between 5 and 15 m, which—influenced by several factors, such as sediment permeability and vegetation type—favors the evapotranspiration of a portion of the water in the USZ before it enters the aquifer. Estimations of the evaporation factors, obtained based on the  $\text{Cl}^-$  balance for different recharge areas taking into consideration several USZ thicknesses, vary between 5.23 and 10.61 (Table 2).

To determine the hydrochemical evolution from the recharge area towards the discharge area, pairs of samples extracted along the trajectory of the groundwater flow were analysed. The models verify that it is the  $\text{Ca}^{2+}/\text{Na}^+$  exchange process that predominates among the

**Table 2** Numerical results of the hydrogeochemical models (values min/max)

Initial/final solution	Evaporation factor	Calcite	$\text{CO}_{2(g)}$	Ca/Na exchange
Rainwater/groundwater recharge	5.23/10.61	0.16/0.21	0.06/0.63	–
Groundwater recharge/groundwater discharge	–	1.27/3.81	0.03/2.71	2.59/4.38

Mass transfer values in mmol/L

hydrochemical characteristics, with values between 2.59 and 4.38 mmol/L (Table 2). Calcite dissolution is higher in the groundwater flow from the recharge areas towards the discharge ones—between 1.27 and 3.81 mmol/L—than during rainwater infiltration—between 0.16 and 0.21 mmol/L (Table 2). These results are consistent with the pH increase observed in the direction of the groundwater flow (Table 1), as calcite dissolution in a closed system with respect to  $\text{CO}_{2(g)}$  consumes the free protons dissolved in the water.

## Conclusions

Phreatic water in the middle and upper basin of the El Pescado creek is characterized by the presence of natural hydrodynamic and hydrochemical conditions scarcely exploited by human activities. An evolution from Ca– $\text{HCO}_3$  type water to Na– $\text{HCO}_3$  type water from recharge areas towards local discharge areas can be inferred.

Processes that define the chemical characteristics and contribute to the hydrochemical evolution are associated with rainwater infiltration,  $\text{CO}_{2(g)}$  and carbonate dissolution, evaporation and cation exchange.

The phreatic aquifer is directly connected to the atmospheric processes that cause water to gain  $\text{CO}_{2(g)}$ . Carbonates, which are abundant in loess sediments, constitute one of the sources of supply of soluble ions to water. The  $\text{SO}_4^{2-}$  and  $\text{Cl}^-$  ions derive from rainwater evaporation. Ion exchange is the predominant process determining groundwater evolution from the recharge areas towards local discharge areas, and it is the main source of  $\text{Na}^+$  supply to water in these sections of the aquifer.

In the case studied, it is possible to define the local discharge areas by means of the presence of Na– $\text{HCO}_3$  type water, associated with the processes of ion exchange. These discharge areas represent local groundwater flows within a plain environment of regional extension. The results may not only be extrapolated to other areas of the phreatic aquifer of the Pampean plain, but also to aquifers with similar hydrogeological characteristics.

## References

- Appelo C, Postma D (2005) *Geochemistry, groundwater and pollution*, 2nd edn. Balkema Publishers, Great Britain
- APHA (American Public Health Association) (1998) *Standard methods for the examination of water and wastewater*, 20th edn. American Public Health Association, American Water Works Association. Water Environment Federation, Washington, DC
- Bonorino G, Albouy R, Carrica J (2001) Hidroquímica de un Acuífero Loésico. *Geoacta* 26:33–45
- Coetsiers M, Walraevens K (2006) Chemical characterization of the Neogene Aquifer, Belgium. *Hydrogeol J* 14:1556–1568
- Fantong WY, Satake H, Ayonghe SN, Aka FT, Asai K (2009) Hydrogeochemical controls and usability of groundwater in the semi-arid Mayo Tsanaga River Basin: far north province, Cameroon. *Environ Geol* 58:1281–1293
- Gaofeng Z, Yonghong S, Chunlin H, Qi F, Zhiguang L (2009) Hydrogeochemical processes in the groundwater environment of Heihe River Basin, northwest China. *Environ Earth Sci*. doi: 10.1007/s12665-009-0175-5
- Hem JD (1985) *Study and interpretation of the chemical characteristics of natural water*, 3rd edn. US Geological Survey Water-Supply Paper 2254
- Kim K, Rajmohan N, Kim HJ, Hwang G, Cho MJ (2004) Assessment of groundwater chemistry in a coastal region (Kunsan, Korea) having complex contaminant sources: a stoichiometric approach. *Environ Geol* 46:763–774
- Kruse E, Laurencena P, Deluchi M, Varela L, Albina L, Rosales E (2003) Relación hidroquímica superficial—subterránea en cuencas de llanura. Noreste de la Provincia de Buenos Aires. I Seminario Hispano—Latinoamericano sobre Temas Actuales de Hidrología Subterránea. Rosario. Universidad Nacional de Rosario. *Memorias*, pp 461–472
- Laurencena P, Kruse E, Rojo A, Deluchi M, Carol E (2005) Variaciones de niveles freáticos en la cuenca del Arroyo El Pescado (Provincia de Buenos Aires). XVI Congreso Geológico Argentino. La Plata, Argentina. Tomo III, pp 725–730
- Magaritz M, Luzier E (1985) Water-rock interactions and seawater-freshwater mixing effects in the coastal dunes aquifer, Coos Bay, Oregon. *Geochim Cosmochim Acta* 49:2515–2525
- Martínez D, Bocanegra E (2002) Hydrogeochemistry and cation-exchange processes in the coastal aquifer of Mar del Plata, Argentina. *Hydrogeol J* 10:393–408
- McLean W, Jankowski J, Lavitt N (2000) Groundwater quality and sustainability in an alluvial aquifer, Australia. In: Sililo O et al (eds) *Proceedings of the 30th congress of the International Association of Hydrogeologists*, Cape Town, South Africa, Balkema, Rotterdam, pp 567–573
- Morgan K, Jankowski J (2004) Saline groundwater seepage zones and their impact on soil and water resources in the Spicers Creek catchment, central west, New South Wales, Australia. *Environ Geol* 46:273–285
- Nadler A, Magaritz M, Mazor E (1980) Chemical reactions of seawater with rocks and freshwater: experimental and field observations on brackish water in Israel. *Geochim Cosmochim Acta* 44:879–886
- Nagaraju A, Suresh S, Killam K, Hudson-Edwards K (2006) Hydrogeochemistry of waters of Mangampeta Barite Mining Area, Cuddapach Basin, Andhra Pradesh, India. *Turk J Eng Environ Sci* 30:203–219
- Parkhurst DL, Appelo CAJ (1999) *User's guide to PHREEQC (version 2)—a computer program for speciation, batch-reaction, one-dimensional transport, and inverse geochemical calculations*. US Geol Surv, Water Resour Invest, Report 99–4259
- Plummer LN, Prestemon EC, Parkhurst DL (1991) An interactive code (NETPATH) for modelling NET geochemical reactions along a flow PATH. US Geol Surv Water Resour Invest 4078
- Quiroz Londoño OM, Martínez DE, Dapeña C, Massone H (2008) Hydrogeochemistry and isotope analyses used to determine groundwater recharge and flow in low-gradient catchments of the province of Buenos Aires, Argentina. *Hydrogeol J* 16: 1113–1127
- Rajmohan N, Al-Futaisi A, Al-Touqi S (2009) Geochemical process regulating groundwater quality in a coastal region with complex contamination sources: Barka, Sultanate of Oman. *Environ Earth Sci* 59:385–398

- Sala JM, Auge M (1973) Presencia de capas filtrantes en el noreste de la Provincia de Buenos.Aires. Su determinación. Actas V Congreso Geológico Argentino Tomo V, pp 185–194
- Teruggi M (1957) The nature and origin of the Argentine loess. *J Sediment Petrol* 27:322–332
- Thornthwaite CW, Mather JR (1955) *The water balance*, vol 8. N.J. Laboratory of Climatology, Publications in Climatology, Centerton, pp 1–104
- Tijani MN (2004) Evolution of saline waters and brines in the Benue-Trough, Nigeria. *Appl Geochem* 19:1355–1365